Analysis of IEEE 802.11p Preamble Insertion in Sidelink C-V2X Signals to Improve Co-Channel Coexistence

Alessandro Bazzi, *Senior Member, IEEE*, Stefania Bartoletti, *Member, IEEE*, Alberto Zanella, *Senior Member, IEEE*, and Vincent Martinez

Abstract—The spectrum scarcity is one of the main challenges of future wireless technologies. When looking at vehicle-toeverything (V2X), this magnifies as spectrum sharing might impact on safety and traffic efficiency. It is therefore of increasing interest to focus on the coexistence of the main access layer V2X technologies in the same geographical region and in the same channels, with particular reference to today's main candidates IEEE 802.11p and sidelink LTE-V2X Mode 4. In this work, in addition to investigating the impact of the reciprocal interference, which is shown to heavily impact especially on the former and in congested channel conditions, a mitigation solution is extensively studied, which is based on the insertion of the IEEE 802.11p preamble at the beginning of the sidelink LTE-V2X transmission. The proposal, which is being discussed also within standardization bodies, requires no modifications to the IEEE 802.11p protocol stack and minor modifications to sidelink LTE-V2X. It is also directly applied to upcoming IEEE 802.11bd and extendable to sidelink 5G-V2X. The paper shows, through analysis and simulations in free-flow and dense scenarios, that the proposal allows a significant improvement of co-channel coexistence in lowly loaded channel conditions and that the improvement is granted also in congested cases when combined with additional countermeasures. Regarding the latter aspect, in particular, different approaches are compared, showing that acting on the congestion control mechanisms is a simple but effective solution.

Index Terms—Connected vehicles; IEEE 802.11p; Sidelink C-V2X; Autonomous mode; Coexistence; Spectrum sharing

I. INTRODUCTION

Spectrum for direct vehicle-to-everything (V2X) communications between vehicle on board units (OBUs) and road side units (RSUs) was reserved in the so-called intelligent transport system (ITS) band around 5.9 GHz in 1999 in the US and in 2008 in Europe. With the aim to improve safety and traffic efficiency, roll-out of vehicles equipped with IEEE 802.11p OBUs is ongoing, mainly in Europe by one large car OEM,¹ together with the deployment of RSUs already covering more than 6000 km of roads.²

- A. Bazzi is with Università di Bologna, Viale Risorgimento 2, 40136 Bologna, Italy (e-mail: alessandro.bazzi@unibo.it).
- S. Bartoletti and A. Zanella are with CNR, Italy (e-mail: {stefania.bartoletti,alberto.zanella}@ieiit.cnr.it).
- A. Bazzi, S. Bartoletti, and A. Zanella are also with CNIT WILAB, Italy. Vincent Martinez is with NXP, Toulouse, France (e-mail: vincent.martinez@nxp.com).
- $^{1}\mathrm{By}$ end of 2021 around 750 000 VW Golf 8 and ID with IEEE 802.11p are predicted to be deployed (source: IHS Markit, 24 Feb 2021).
- ²Numbers related to commercially deployed RSUs in Europe in 2019 (source: C-Roads at the C2C-CC Forum, November 2020).

It is however clear that the radical change enabled by short-range connectivity will be visible only when the market penetration will increase significantly. Among the reasons for the delayed roll-out, despite solutions are available and tested also on a large scale, there is the technical debate involving the two families of standards which have been defined for this scope, i.e., the one based on IEEE 802.11 and the other based on the sidelink technologies designed by the Third Generation Partnership Project (3GPP) for V2X in LTE and 5G. Given the failed attempts to mandate either technology,³ one of the main open issues is the investigation of their coexistence in the same channels, namely spectrum sharing, and solutions to mitigate the reciprocal interference.

Co-channel coexistence of different technologies is in general a well known and investigated issue. For example, all technologies using the industrial, scientific and medical (ISM) bands need to apply some mechanism to limit the interference produced to possible coexisting ones. Just to mention a few, ZigBee and WiFi adopt a carrier sensing multiple access with collision avoidance (CSMA/CA) mechanism, Bluetooth implements frequency hopping spread spectrum (FHSS), and LoRa implements chirp spread spectrum (CSS). Additionally, proposals to further mitigate the reciprocal interference have been presented in the literature (e.g., [1], [2]), also considering Wi-Fi and LTE in unlicensed ISM bands [3], [4]. Nevertheless, co-channel coexistence represents a new topic when discussing the ITS band, which is nowadays associated with IEEE 802.11p and sidelink LTE-V2X (simply LTE-V2X in the following, for conciseness). To the best of our knowledge, such topic is indeed considered only in a few early works [5], [6] and the study published in the ETSI TR 103 766 [7], where a few solutions to reduce the impact of inter-technology interference are proposed and preliminary investigated.

This paper focuses on a solution to mitigate reciprocal interference between IEEE 802.11p and LTE-V2X communications consisting in the insertion of an easy-to-store and fixed short preamble to the LTE-V2X signal, which improves IEEE 802.11p awareness and reduces the inter-technology collision probability. As this preamble sequence is fixed and predefined, LTE-V2X stations do not need to implement the IEEE 802.11p standard; they could directly use a pre-

³In the US, a proposed rule was issued on January 2017, which ended with a stalemate. In Europe, a Delegated Act was proposed by the European Commission in March 2019, which was however rejected by the European Parliament in July 2019.

recorded sequence. Additionally, this solution appears by design compatible with IEEE 802.11bd and also extendable to sidelink 5G-V2X. The preamble insertion is part of one of the mitigation methods discussed in [7], used together with a time domain sharing mechanism that distinguishes between LTE-V2X and ITS-G5 time-slots. However, the insertion of the preamble has never been considered as a standalone solution and a formal analysis of its implications is still missing.

After recalling the main aspects of both technologies and discussing the implications of their co-channel coexistence in Section II, we detail the concept of preamble insertion in Section III. We then investigate its performance through Sections IV and V. In particular:

- We first focus on a free-flow scenario in Section IV and introduce a mathematical model for the analysis of the IEEE 802.11p preamble insertion showing the significant reduction of inter-technology collisions;
- Then we move to a denser scenario in Section V and share results derived exploiting an open source simulator, confirming the validity of the approach for uncongested scenarios; furthermore, some possible approaches are compared to deal with the congested cases, showing that acting on the congestion control procedures of sidelink LTE-V2X is more effective than others more complex.

Our conclusions are finally drawn in Section VI.

II. TECHNOLOGIES AND COEXISTENCE ISSUES IN BRIEF

In this section, the two technologies are briefly described and the issues that arise when they are both adopted in the same channel in the same geographical area are discussed.

A. IEEE 802.11p and related standards

IEEE 802.11p, completed in 2010 and now part of IEEE 802.11-2020 [8], relies on orthogonal frequency division multiplexing (OFDM) at the physical (PHY) layer and CSMA/CA at the medium access control (MAC) layer. In the US, it is used for the lower layers of the protocol stack denoted as wireless access in vehicular environment (WAVE), which includes the IEEE 1609 standards and is completed at the higher layers by documents from SAE. In Europe, it is used for the ITS-G5 access layer, which has been defined by ETSI together with a number of standards dealing with all the layers of the protocol stack. Currently, an evolution is under definition as IEEE 802.11bd, which completion is expected by 2022.

Adopting CSMA/CA, IEEE 802.11p is by design an asynchronous fully distributed ad-hoc protocol. Each time a station needs to transmit, it senses the medium for a given duration and either transmits if the channel is sensed idle or differs until the ongoing transmission is concluded. When the transmission starts, all subcarriers are used for a time that depends on the payload size and the adopted modulation and coding scheme (MCS). In V2X, for the time being messages are sent in broadcast mode and thus an access-layer acknowledgment by the receiver(s) is not foreseen.

The access mechanism of IEEE 802.11p and the channel usage are exemplified in Fig. 1(a). More details about IEEE 802.11p can be found for example in [9], [10].

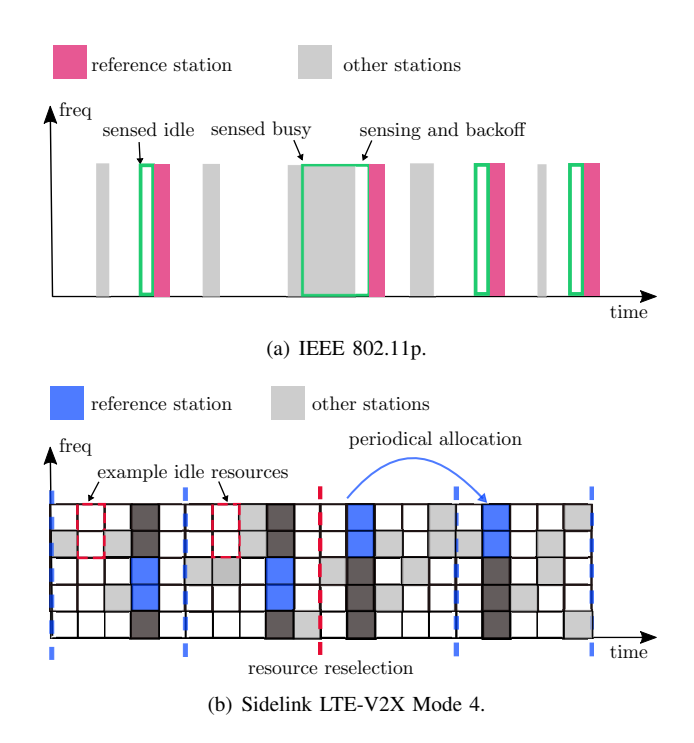
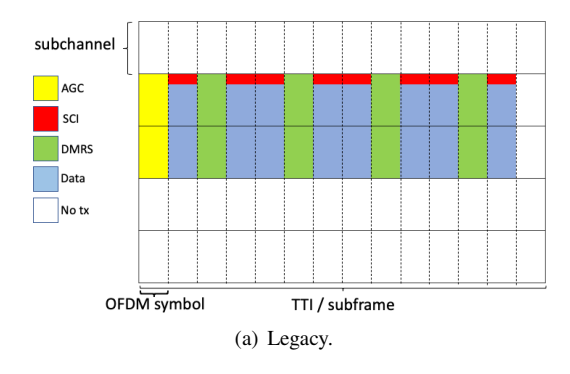


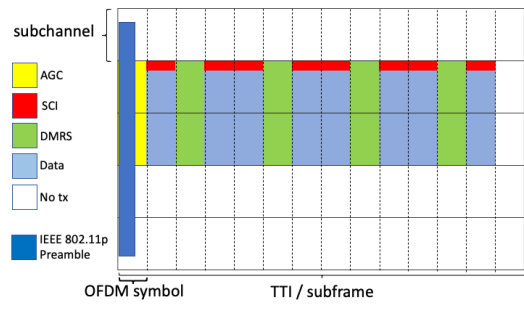
Fig. 1. Exemplification of the medium access mechanisms.

B. Sidelink C-V2X and LTE-V2X Mode 4

Since Release 14, freezed in 2016, the 3GPP has introduced LTE-V2X, then indicated as part of the so-called cellular-V2X (C-V2X). C-V2X is indeed an umbrella covering both LTE and 5G, and including downlink/uplink (Uu interface) and sidelink (PC5 interface) communications. Focusing on sidelink, the resource allocation can be either performed by the network, called Mode 3 in LTE and Mode 1 in 5G, or autonomously by the stations, called Mode 4 in LTE and Mode 2 in 5G. In this paper, sidelink LTE-V2X Mode 4 is considered, as it is the solution currently under consideration for the ITS band.

LTE-V2X relies at the PHY and MAC layers on single carrier frequency division multiple access (SC-FDMA), with a resource granularity of a transmission time interval (TTI) in the time domain and a subchannel in the frequency domain. The TTI, also called subframe, is 1 ms long, while one subchannel occupies a predefined number of physical resource blocks (PRBs) [11], with a PRB corresponding to 12 subcarriers over 180 kHz. Each transmission therefore lasts 1 ms and occupies a portion of the bandwidth that depends on the payload size and the adopted MCS. In LTE-V2X, each message can be transmitted two times thanks to the so-called hybrid automatic request (HARQ), which is a blind retransmission mechanism activated by default although regulated depending on self channel usage. The allocation process performed at the MAC layer has been designed assuming periodic messages and relies on a sensing-based semi-persistent scheduling (SB-SPS) approach: a station with a message to transmit, looks at the occupation of the resources in the last time window of 1 s, based on measurements and information carried by the sidelink control informations (SCIs) associated to each packet, to infer what will be the occupation in the future. Once the resource is allocated, no further sensing of the channel is done before transmitting, and the same resource is used periodically for





(b) With IEEE 802.11p preamble insertion.

Fig. 2. Comparison between legacy and preamble insertion. Example of an LTE-V2X transmission using two of five subchannels, assuming adjacent allocation of the sidelink control information. Each figure represents a signal using two of the five subchannels in frequency for the 14 OFDM symbols forming one time transmission interval. AGC for automatic gain control, SCI for sidelink control information, DMRS for demodulation reference signals.

a given duration, before repeating the procedure, which is independent to the measurements.

The details of Mode 4, which is exemplified in Fig. 1(b) and has been extensively studied in the last few years, can be found for example in [12]–[14].

C. Co-channel coexistence

When looking at co-channel coexistence, we can note that IEEE 802.11p, through the use of CSMA/CA, also known as *listen-before-talk*, is inherently designed to limit its interference towards other technologies. Differently, LTE-V2X is derived from technologies that do not normally need to cope with co-channel coexistence and are not designed to take this aspect into account. As already remarked, an LTE-V2X station adopting Mode 4 starts a transmission using resources that were previously allocated, without any additional procedure. The issue is further exacerbated under high channel load conditions, with the risk of strong unfairness due to the fact that LTE-V2X tends to use most of the resources, while IEEE 802.11p tends to postpone and eventually reduce its access.

Another potential issue, worth mentioning although not deepened in this work, is caused by the presence of a gap at the end of the LTE transmission used for switching from transmission to reception mode, which leads to around 71.4 μ s of idle channel between two consequent LTE-V2X transmissions. In some cases, ⁴ that time might be longer than the access time of IEEE 802.11p and the sensing mechanism would fail to identify the use by LTE-V2X stations of subsequent TTIs.

III. IEEE 802.11P PREAMBLE INSERTION

An IEEE 802.11p transmission starts with a preamble of 40 μ s, which includes a short and a long training sequence, lasting each for 16 μ s, and the Signal Field OFDM symbol, lasting 8 μ s. Such symbol adopts BPSK and 1/2 coding rate, carrying 24 useful bits over 48 data subcarriers. From those 24 bits, the duration of the remaining signal can be derived. Please remark that two signals of the same duration will start with exactly the same preamble.

In legacy LTE-V2X, the signal, which occupies one TTI of 1 ms, is divided into 14 OFDM symbols of approximately

⁴For example with the parameters defined in Europe for high-priority decentralized environmental notification messages (DENMs) in ITS-G5.

71.4 μ s. As represented in Fig. 2(a), the first symbol is used for automatic gain control (AGC) (it carries a copy of the second symbol), 4 are used for demodulation reference signals (DMRSs), 8 for data, and the last one is left empty to allow switching from transmission to reception mode. In Fig. 2(a), the channel is organized in five subchannels in compliance with [15] and, as an example, the signal occupies two of them.

The idea of the IEEE 802.11p preamble insertion is to replace, as shown in Fig. 2(b), the first 40 μ s of the LTE-V2X signal with an IEEE 802.11p preamble indicating the occupation of the channel for 1 ms.⁵ As mentioned, the first part of the LTE-V2X signal is anyway carrying redundancy and the added preamble is always the same, thus stored IQ samples could be used to generate the signal without additional complexity to the LTE-V2X transmitter. The data-rate of LTE-V2X is not reduced and the LTE-V2X station does not need to implement the IEEE 802.11p standard. Since the preamble signal is strictly regulated and is always the same for any station at any point of time, the presence of concurrent time-synchronized LTE-V2X signals will have the same impact on the preamble decoding as multiple paths, just like for single frequency network type of systems.

Two advantages are obtained with the considered approach. First, the LTE-V2X occupation of 1 ms is indicated as part of the *signal field* of the preamble and thus the gap at the end of the TTI does not cause CSMA/CA to sense the channel as idle. Second, more importantly, it significantly reduces the received power at which IEEE 802.11p assumes the channel as busy; in fact, from the -65 dBm of the clear channel assessment (CCA) threshold, which is used when an undecodable signal is received, the minimum power is reduced to a level that depends on the implemented receiver and can be reasonably assumed around -100 dBm.⁶ Please note that simply reducing the CCA threshold to a lower level would not lead to the same result; the threshold was in fact optimized in order to avoid false detection of unexpected signals, including for example spurious emissions from adjacent channels.

⁵A different proposal was also to place the header in the empty symbol prior to the subframe.

⁶The value of -100 dBm, which is in agreement with what obtained in offthe shelf devices, corresponds to a signal to noise ratio (SNR) of -2 dB with a noise figure of 6 dB. A slightly higher value is used here for performance evaluation, as motivated in Section V-A. Example reference is the Cohda MK5, fccid.io/2AEGPMK5RSU/Users-Manual/User-Manual-2618067.pdf A difference compared to current specifications is that the addition of the preamble, as shown in Fig. 2(b), causes some power to be transmitted over all subchannels at the beginning of the TTI, even when part of the bandwidth is used for the rest of the TTI. This, in principle, might alter the SB-SPS process of LTE-V2X. However, the signal is transmitted only for $40~\mu s$ over the 1 ms TTI and thus the impact is negligible, as later demonstrated in Section V-B.

An additional advantage of the proposed solution is its applicability to the newer IEEE 802.11bd and sidelink 5G-V2X. In IEEE 802.11bd, the same preamble is already part of the specifications by design. In the case of 5G-V2X, nothing is expected to change from LTE-V2X if the same numerology is used, i.e., with same subcarrier spacing of 15 kHz and same TTI of 1 ms. The methodology looks also applicable when the subcarrier spacing is increased to 30 kHz and the TTI reduced to 0.5 ms: in such a case, each OFDM symbol lasts about 35 μ s, but part of the gap from the previous symbol could be used to accommodate the 40 μ s preamble. Only in case that a higher subcarrier spacing was used, which is anyway not expected for channels of 10 MHz in the ITS band, more than one symbol would be necessary, which might cause a reduction of the useful data-rate.

IV. IMPACT IN THE FREE-FLOW SCENARIO

In this section, the impact of the preamble insertion is investigated in a low-traffic scenario. A model is developed to this aim, providing an insight on the ability of the proposal to reduce the collisions between IEEE 802.11p and LTE-V2X transmissions coexisting in the same channel.

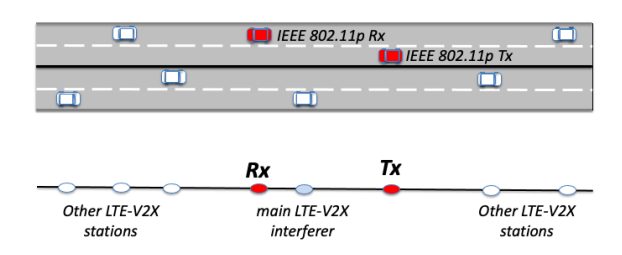
A. Scenario and assumptions

Given the low density, the free-flow scenario is reproduced by focusing on a single IEEE 802.11p transmission interfered by a variable number of LTE-V2X transmissions. The impact of the preamble insertion is assessed here in terms of packet reception probability (PRP) of the IEEE 802.11p link, which is the technology mostly penalized by co-channel interference [5], [7]. Additional performance metrics are assessed in Section V through simulations in denser scenarios.

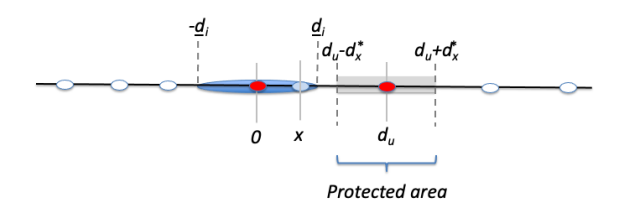
The instant when the IEEE 802.11p packet reaches the access layer transmission buffer is randomly chosen and not aligned with the subframe structure of LTE; the duration of the channel sensing, lasting for an arbitration inter-frame space (AIFS), plus the packet transmission are assumed to last for less than 1 ms.⁷ The performance is calculated in terms of PRP varying the IEEE 802.11p source-destination distance and the average number of LTE-V2X transmissions per meter per second.

The model developed for this scenario is based on the following approximations:

 As represented in Fig. 3(a), the highway scenario is approximated as a straight line, thus the LTE-V2X nodes correspond to a 1-D Poisson point process (PPP) distribution (like, for example, the models adopted in [16]–[18]);



(a) Example with both 2-D and 1-D representation.



(b) Corresponding parameters.

Fig. 3. Free-flow scenario and parameters used in the model.

- Given the low density scenario, only the strongest LTE-V2X interference source is assumed in each subframe; this approximation is adopted by several articles such as, for example, [19];
- The correct reception is modeled through a threshold model, meaning that the packet is correct when the signal to noise and interference ratio (SINR) is above the threshold and incorrect when it is below; fading effects are included in the setting of the threshold.

It is to note that the analysis is validated by simulations where the channel is modeled in more details and includes log-normal large-scale fading (shadowing), and packet error rate (PER) vs. SINR curves which take small-scale fading into account.

B. Model definition

Considering a 1-D scenario as represented in Fig. 3(b), the IEEE 802.11p receiver is assumed in position 0. Without lack of generality, the IEEE 802.11p transmitter is located on the right of the receiver, in position $d_{\rm u}$, i.e. the distance between the transmitter and the receiver is $d_{\rm u}$. There are λ average LTE-V2X transmissions per meter per second.

Given that no retransmissions are allowed in IEEE 802.11p, assuming the interference from the generic LTE-V2X signal as white and Gaussian, the PRP can be written as

$$\mathbb{P}_{PR} = 1 - f_{PER} \left(\gamma \right) \tag{1}$$

where $f_{\rm PER}\left(\gamma\right)$ is the PER deriving from the average SINR calculated as $\gamma=P_{\rm R}/\left(P_{\rm N}+P_{\rm I}\right),\ P_{\rm R}=P_{\rm 11p}G_{\rm t}G_{\rm r}/L(d_{\rm u})$ is the average received power, $P_{\rm 11p}$ is the transmission power of IEEE 802.11p stations, $G_{\rm t}$ and $G_{\rm r}$ are the antenna gains at the transmitter and the receiver, respectively (assumed the same for all transmitters and receivers for simplicity), $P_{\rm N}$ is the average noise power, and $P_{\rm I}=P_{\rm LTE}G_{\rm t}G_{\rm r}/L(d_{\rm i})$ is the average interfering power from an LTE-V2X node transmitting with

⁷1 ms corresponds to approximately 700 bytes adopting the default MCS 2.

power P_{LTE} at a distance d_{i} from the receiver. For the sake of conciseness, in (1) d_{u} and d_{i} are left implicit in γ .

The packet under evaluation is generated at a generic instant within what we call the *current TTI*. The subframe just following is hereafter denoted *subsequent TTI*. If the channel is sensed idle and the transmission starts, depending on the generation instant the transmission is either entirely performed within the current TTI or overlaps partially with the subsequent TTI. Denoting as $t_{\rm pck}$ the IEEE 802.11p duration including the AIFS and as $t_{\rm TTI}$ the duration of one TTI, the transmission is entirely contained in the current TTI with probability $\mathbb{P}_{\rm c} = (t_{\rm TTI} - t_{\rm pck})/t_{\rm TTI}$, and partially occupies the subsequent one with probability $\mathbb{P}_{\rm sq} = 1 - \mathbb{P}_{\rm c}$.

Given that the position of the interfering LTE-V2X node and the selected TTI are independent, the distribution of the nodes using the current TTI is a 1-D PPP process with density $\lambda_{\rm TTI} = \lambda/N_{\rm TTI}$, where $N_{\rm TTI} = 1/t_{\rm TTI}$ is the number of TTIs in one second. Similarly, the distribution of the nodes using the subsequent TTI is also a 1-D PPP process with density $\lambda_{\rm TTI}$, independent from the previous one.

For the properties of PPP distributions, the strongest LTE-V2X interferer in the current TTI is in the position x (positive or negative), thus at distance |x| from the destination, with probability $\mathbb{P}_{\rm d}(x) = \lambda_{\rm TTI} e^{-2\lambda_{\rm TTI}|x|}$. Similarly, the strongest LTE-V2X interferer in the subsequent TTI is in the position y from the destination with probability $\mathbb{P}_{\rm d}(y) = \lambda_{\rm TTI} e^{-2\lambda_{\rm TTI}|y|}$.

We call the maximum distance at which the interfering signal can be sensed by the IEEE 802.11p transmitter as protected range and denote it as $d_x^* = L^{-1}(P_{\mathrm{R},x}^*)$, where $P_{\mathrm{R},x}^*$ is the minimum received power to set the channel as busy. The area from $d_\mathrm{u}-d_x^*$ and $d_\mathrm{u}+d_x^*$ is called protected area (see Fig. 3(b)). A transmission from an LTE-V2X node in the protected area is sensed by the IEEE 802.11p transmitter during the carrier sense procedure; thus, if the main LTE-V2X interferer during the current TTI is within the protected area, then the IEEE 802.11p station will defer its transmission.

Depending on the position of the main LTE-V2X interferer in the current TTI and the instant when the IEEE 802.11p transmission ends, three cases are possible: (i) the LTE-V2X interferer is within the protected area, in which case the transmission is deferred to the first TTI during which the main LTE-V2X interferer is outside the protected area; this event occurs with probability \mathbb{P}_{busy} and causes a PRP equal to $\mathbb{P}_{PR|busy}$; (ii) the LTE-V2X interferer is outside the protected area and the IEEE 802.11p transmission ends within the current TTI; this event occurs with probability $\mathbb{P}_{c\text{-idle}}$ and causes a PRP equal to $\mathbb{P}_{PR|c}$; and (iii) the LTE-V2X interferer is outside the protected area and the IEEE 802.11p transmission ends in the subsequent TTI; this event occurs with probability $\mathbb{P}_{sq\text{-idle}}$ and causes a PRP equal to $\mathbb{P}_{PR|sq}$. For the law of total probability, it is

$$\mathbb{P}_{PR} = \mathbb{P}_{busy} \mathbb{P}_{PR|busy} + \mathbb{P}_{c\text{-}idle} \mathbb{P}_{PR|c} + \mathbb{P}_{sq\text{-}idle} \mathbb{P}_{PR|sq} . \tag{2}$$

The probability that the channel is sensed busy by the

reference transmitter during the current TTI is

$$\mathbb{P}_{\text{busy}} = \int_{d_{\mathbf{u}} - d_{x}^{*}}^{d_{\mathbf{u}} + d_{x}^{*}} \mathbb{P}_{\mathbf{d}}(x) dx = \frac{1}{2} \left[(1 - e^{-2\lambda_{\text{TII}}(d_{x}^{*} + d_{\mathbf{u}})}) + \text{sign}(d_{x}^{*} - d_{\mathbf{u}}) \cdot (1 - e^{-2\lambda_{\text{TII}}|d_{x}^{*} - d_{\mathbf{u}}|}) \right] \tag{3}$$

where ${\rm sign}(x)$ is the sign function, returning +1 if $x\geq 0$ and -1 if x<0. The sign function and absolute value in the second term of (3) account for the possibility that the protected area is partly in the negative axis (i.e., $d_x^*>d_{\rm u}$), or not. If the current TTI is sensed busy, the IEEE 802.11p station will differ its transmission to the first TTI in which the main LTE-V2X interferer is outside the protected area. Given the independence of the distributions of the LTE-V2X nodes in the TTIs, in this case the PRP is equal to

$$\mathbb{P}_{\text{PR}|\text{busy}} = \frac{1/2}{1 - \mathbb{P}_{\text{busy}}} \left[\left(e^{-2\lambda_{\text{TTI}} \cdot \left(\max\{\underline{d_i}, (d_x^* - d_u)\} \right)} \right) + \left(e^{-2\lambda_{\text{TTI}} \cdot \left(\max\{\underline{d_i}, (d_x^* + d_u)\} \right)} \right) \right]$$
(4)

where $\max\{x,y\}$ is a function that returns the maximum between x and y, and $\underline{d_i}$ is the minimum distance corresponding to the maximum interference to correctly receive the packet; please note that whereas d_x^* is independent on d_u , $\underline{d_i}$ varies with d_u . The derivation of (4) is detailed in Appendix A.

The same PRP is also obtained if the reference transmitter is unable to sense the LTE signal in the current TTI and it ends in the current TTI. Such an event, occurring with probability

$$\mathbb{P}_{\text{c-idle}} = (1 - \mathbb{P}_{\text{busy}}) \, \mathbb{P}_{\text{c}} \tag{5}$$

is thus characterized by PRP equal to

$$\mathbb{P}_{PR|c} = \mathbb{P}_{PR|busy} . \tag{6}$$

In the case the reference transmitter is unable to sense the LTE signal in the current TTI and it ends in the subsequent TTI, which occurs with probability

$$\mathbb{P}_{\text{sq-idle}} = 1 - \mathbb{P}_{\text{busy}} - \mathbb{P}_{\text{c-idle}} = (1 - \mathbb{P}_{\text{busy}}) (1 - \mathbb{P}_{\text{c}}) \quad (7)$$

the PRP is a function of both the interference in current TTI and that in subsequent TTI. Please note that the ability of the reference transmitter to sense or not the LTE transmissions in the subsequent TTI is irrelevant, as the IEEE 802.11p transmission has been already started when the LTE-V2X transmission begins. The exact expression, reported in Appendix B, includes a triple integral. However, approximating the interference as entirely caused by the LTE-V2X transmission that overlaps most with the reference transmission, we obtain

$$\mathbb{P}_{PR|sq} \simeq \frac{\mathbb{P}_{PR|busy}}{2} + \frac{\mathbb{P}_{PR|unpr}}{2} \tag{8}$$

having defined with

$$\mathbb{P}_{\mathsf{PR}|\mathsf{unpr}} = e^{-2\lambda_{\mathsf{TTI}}d_x^*} \tag{9}$$

the PRP in the presence of interference without the sensing procedure (thus, unprotected). The derivation of (8) and (9) is detailed in Appendix B.

As a consequence of (5), (6), (7), and (8), the PRP in (2) can be rewritten as

Free-flow scenario							
Scenario	Highway, approximated as 1-D						
Density	Variable						
Average transmissions	Variable						
Denser scenarios							
Scenario	3+3 lanes highway, 2 km straight road [20]						
Density	Variable						
Mobility	Gaussian distributed speed, with average						
	70 km/h and std. dev. 7 km/h						
Packet periodicity	Following CAM rules [21]						
Common settings							
Channels	ITS bands at 5.9 GHz						
Bandwidth	10 MHz						
Transmission power density	13 dBm/MHz						
Antenna gain (tx and rx)	3 dB [5]						
Noise figure	6 dB [5]						
Propagation model	WINNER+, Scenario B1, line-of-sight [20]						
Shadowing	Variance 3 dB, decorr. dist. 25 m [20]						
Packet size	350 B [22]						
IEEE 802.11p							
MCS	2 (QPSK, 1/2), PER=0.5@SINR=1.02 dB						
Duration of the initial space	$110 \ \mu s \ [23]$						
Random backoff	$[0 \div 15] \cdot 13 \ \mu s \ [23]$						
Carrier sense threshold	-65 dBm						
Preamble detection threshold	-98.8 dBm (see Section V-A)						
Congestion control	ETSI DCC [24] (see Appendix C)						
Sidelink LTE-V2X Mode 4							
MCS	11 (16-QAM, 0.41), PER=0.5@SINR=5.15 dB						
Subchannel size	10 resource block pairs [15]						
Number of subchannels	5						
Subchannels per packet	2						
Configuration	Adjacent						
Keep probability	0.5						
Allocation periodicity	100 ms [25]						
Subchannel sensing threshold	-110 dBm						
Congestion control	ETSI CC for LTE-V2X [26] (see Appendix C)						
HARQ	Blind retransmission if CC allows						

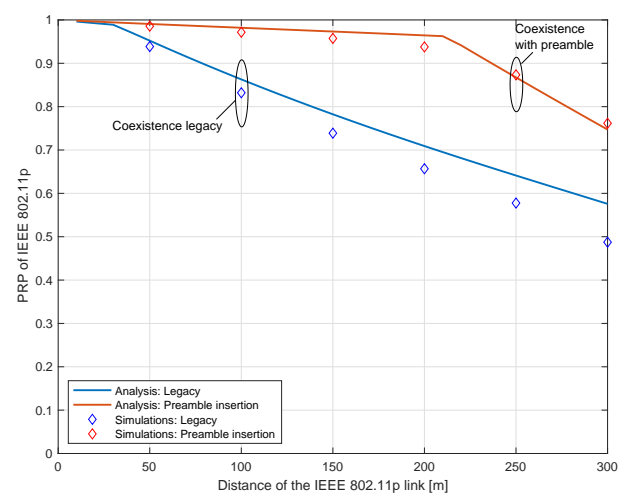
$$\begin{split} \mathbb{P}_{PR} &\simeq & \mathbb{P}_{busy} \mathbb{P}_{PR|busy} + \mathbb{P}_{c\text{-idle}} \mathbb{P}_{PR|busy} + \mathbb{P}_{sq\text{-idle}} \left(\frac{\mathbb{P}_{PR|busy}}{2} + \frac{\mathbb{P}_{PR|unpr}}{2} \right) \\ &= \left(1 - \frac{\mathbb{P}_{sq\text{-idle}}}{2} \right) \mathbb{P}_{PR|busy} + \left(\frac{\mathbb{P}_{sq\text{-idle}}}{2} \right) \mathbb{P}_{PR|unpr} \;. \end{split} \tag{10}$$

By using the results of (3), (4), and (9), (10) gives a closed-form expression of the PRP as a function of d_u and λ .

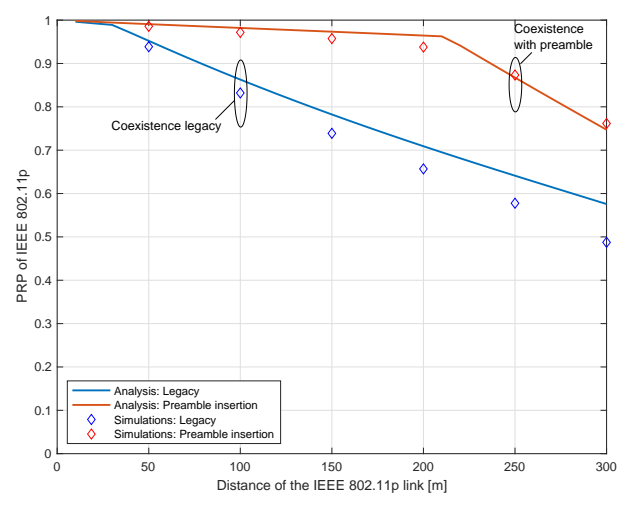
C. Results in the free-flow scenario

Fig. 4 shows the performance results obtained using the proposed model and assuming the settings listed in Table I. The $\underline{\gamma}$ adopted in the analysis corresponds to the SINR of the PER vs. SINR curve used in the simulations with PER equal to 0.5. The WINNER+, scenario B1 model is used for the path-loss, which is approximated in the analysis as $L(d_{\rm u})[dB] = \alpha + 10 \cdot \beta \cdot \log_{10}(d_{\rm u})$, where $\alpha = 20.06$ dB and $\beta = 4$. The protected range corresponds to approximately 55 m in the legacy case, due to $P_{\rm R,x}^* = -65$ dBm, and approximately 390 m with the addition of the preamble, due to $P_{\rm R,x}^* = -98.8$ dBm.

In Fig. 4(a), the PRP of the IEEE 802.11p link is shown varying the transmitter-receiver distance with 1000 LTE-V2X transmissions per km per second (which corresponds, for example, to 50 vehicles per km generating a message every 100 ms and transmitting it twice with blind retransmissions). The coexistence between the two standard (legacy) technologies is compared with that of LTE-V2X with the preamble



(a) Packet reception probability of the IEEE 802.11p link vs. the link distance, with 1000 LTE-V2X transmissions per kilometer per second.



(b) Packet reception probability of the IEEE 802.11p link at 200 m vs. average LTE-V2X transmissions per kilometer per second.

Fig. 4. Free-flow scenario. Impact of the preamble insertion on the packet reception probability of one IEEE 802.11p transmission interfered by coexisting LTE-V2X transmissions.

insertion and standard IEEE 802.11p. Despite the approximations adopted, analysis and simulations show a very similar trend. Looking at Fig. 4(a) and comparing the PRP with legacy and with preamble insertion, the improvement due to the preamble insertion is clear. The PRP improvement granted by the preamble insertion starts reducing at nearly 200 m, which approximately corresponds to the distance for which $\underline{d_i}$ equals $d_x^* - d_u$. This value impacts directly on (4): until $\underline{d_i} < d_x^* - d_u$, the interferer is in the protected area, thus the channel is sensed as busy and the transmission is deferred; when $\underline{d_i} > d_x^* - d_u$, the channel is sensed as idle and the transmission starts immediately, possibly ending in a collision.

In Fig. 4(b), the PRP at 200 m is shown varying the density of LTE-V2X transmissions. Analysis and simulations still show a similar trend. Comparing the performance with legacy and preamble insertion, the success of the proposed approach to reduce the burden of LTE-V2X interference to IEEE 802.11p is also clear. Inherently, the results indicate a reduction of the overlapping between IEEE 802.11p and LTE-

V2X signals, which also improves the LTE-V2X reliability, as confirmed in the next section.

V. IMPACT IN DENSER SCENARIOS

In this section, results are discussed from large-scale simulations obtained through the open-source WiLabV2Xsim [27].⁸

A. Simulation settings

The main settings are detailed in Table I. The physical layer is abstracted as follows: for each potentially received packet, the average SINR is calculated by taking into account the average interference from all the other nodes. The WINNER+, B1, model is adopted for the path-loss, with log-normal correlated large scale fading (shadowing) as better detailed in [5]. Once the SINR is calculated, the correct reception of each packet is statistically drawn from the PER vs. SINR curves shown in [5], which take into account the impact of small-scale fading. To take into account that the preamble is more protected than the packet, it is assumed correctly decoded when the SINR is above the value in the curves used for data corresponding to 0.9 PER; this means approximately -0.8 dB SINR and thus a minimum received power of nearly -98.8 dBm to successfully decode the preamble in the absence of interference. This value is in good agreement with common IEEE 802.11p receivers. The power of the preamble received concurrently from more sources is assumed to combine positively thanks to the properties of OFDM.

The following metrics are considered for both technologies:

- Packet reception ratio (PRR), computed as the average ratio between the number of vehicles at a certain distance from the transmitter that are correctly decoding a packet and the overall number of vehicles at the same distance; PRR is calculated with a granularity of 10 m;
- Data age (DA), corresponding to the time elapsed from the generation of a correctly received packet and the next correctly decoded one by the same receiver from the same transmitter; it implicitly accounts for the allocation delay and the correlation among errors; DA is evaluated for all transmissions within 400 m.

B. Considerations with either technology alone

IEEE 802.11p is not at all affected by the proposal when deployed alone. Differently, the addition of the preamble might in principle influence the LTE-V2X behavior when deployed alone. In fact, the preamble insertion implies that some power is distributed over the entire bandwidth at the beginning of an LTE-V2X signal, no matter how large is the portion occupied by the rest of the signal (see Fig. 2). Thus, a slightly higher power is measured by the neighbouring LTE-V2X stations in the subchannels of the same TTI which are not used. In turn, the power added on unused subchannels of an used subframe might in principle affect the SB-SPS process of LTE-V2X.

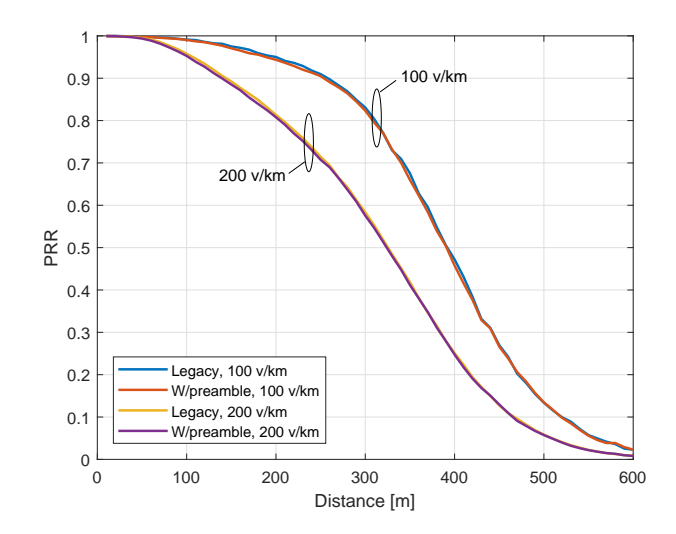


Fig. 5. Performance of LTE-V2X only, with the preamble insertion and without (legacy). Highway scenario, 100 and 200 v/km.

However, the power increment in the unused subchannels is very small, as it is slightly more than 4% of the power in the used subchannels (40 μ s over 13 OFDM symbols). The curves shown in Fig. 5, which refer to a scenario with 100 or 200 LTE-V2X stations per km, both with and without preamble insertion, demonstrate that such an effect is indeed negligible.

C. Performance of preamble insertion without any additional modification

The impact of preamble insertion from the point of view of both technologies is shown in Fig. 6, which compares, in a scenario with 100 vehicles per technology per km, the following cases:

- *IEEE 802.11p/LTE-V2X only*: the vehicles are equipped with the indicated technology; this case is used as a term of comparison, without inter-technology interference;
- Coexistence legacy, where IEEE 802.11p and LTE-V2X legacy stations share the channel;
- Coexistence legacy, periodic traffic, where the two legacy technologies share the channel and the traffic generation is strictly periodic; in this case, in order to have a similar average number of packets per station per second, the generation interval of both technologies and the allocation period of LTE-V2X are set to 200 ms;
- *Coexistence w/preamble*, where they share the same channel and the preamble insertion is used in LTE-V2X.

The case with periodic traffic is used to investigate what happens if the SB-SPS of LTE-V2X is able to sense the use of the channel by IEEE 802.11p stations, which corresponds to the inter-technology interference mitigation proposed in [5].

Specifically, Figs. 6(a) and 6(b) provide the PRR varying the transmitter-receiver distance, with focus on IEEE 802.11p and LTE-V2X, respectively. Looking at Fig. 6(a) and comparing the curves with IEEE 802.11p alone and coexistence legacy, the presence of LTE-V2X is shown to significantly reduce the PRR. The use of either a periodic packet generation or the preamble insertion allow a significant mitigation of the intertechnology interference. Similar considerations can be inferred

⁸The simulator is available at https://github.com/V2Xgithub/WiLabV2Xsim. The modifications done for the present paper will be included in the future releases of the simulator and in the meanwhile provided upon request.

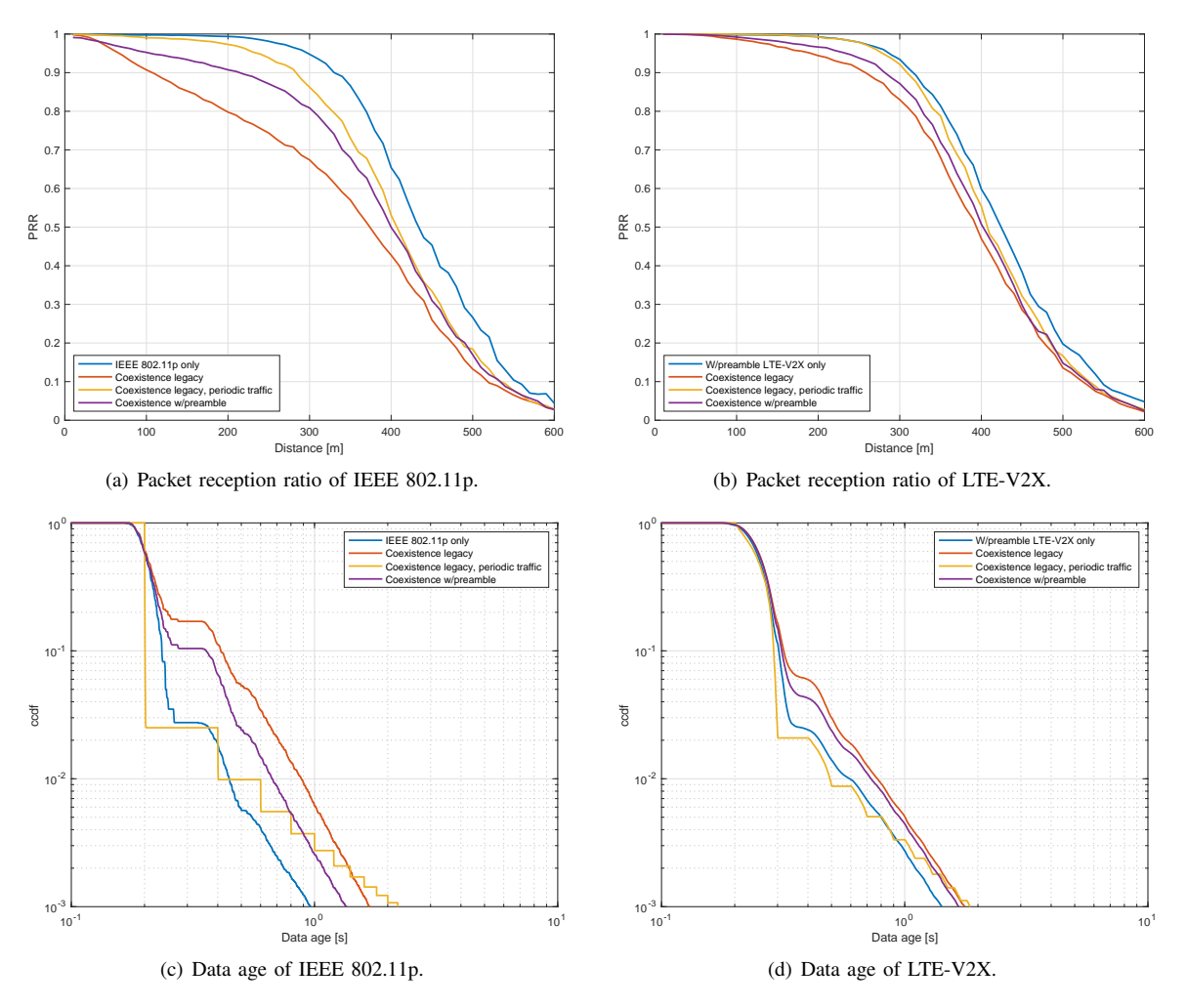


Fig. 6. Comparison between: (i) single technology with 50 v/km; (ii) coexistence of 50 IEEE 802.11p and 50 LTE-V2X v/km without any modifications; (iii) coexistence of 50 IEEE 802.11p and 50 LTE-V2X v/km without any modifications but with periodic traffic; (iv) coexistence of 50 IEEE 802.11p and 50 LTE-V2X v/km with the preamble insertion.

also from Fig. 6(b) when referring to LTE-V2X, although the negative impact of IEEE 802.11p on the PRR of LTE-V2X is smaller than in the reverse case.

In Figs. 6(c) and 6(d), the complementary cumulative distribution function (ccdf) of the DA is shown referring to IEEE 802.11p and LTE-V2X, respectively. These plots confirm the conclusions derived from Figs. 6(a) and 6(b), except for the case of periodic packet generation. In such case, in fact, the periodical transmissions cause consequent collisions to occur more frequently, which turns out in a higher DA. Indeed, if we look at a ccdf of 0.001 (DA occurring with probability 0.001 or lower), we notice that the largest value is the one corresponding to the periodical generation. Also from this perspective, the preamble insertion shows an improvement compared to the legacy coexistence.

Similar results are also observed varying the density of the vehicles, not shown here for the sake of conciseness. A comparison of the coexistence with legacy and with preamble insertion for various densities can in any case be obtained looking at the first two bars of the series shown in Fig. 7. In Figs. 7(a) and 7(b), the maximum distance with PRR higher than 0.9 is shown varying the density of the scenario; we can

observe that the use of the preamble outperforms the legacy case, with the only exception of IEEE 802.11p with 150+150 v/km, where they behave similarly. Figs. 7(c), and 7(d) show the minimum DA with probability lower than 0.001. Also in this case, the use of the preamble leads to a lower DA for both technologies, with the only exception of IEEE 802.11p with 150+150 v/km, as motivated in the next subsection.

D. Considerations on the CBR

In Table II, per each simulated density and case, and for both technologies, the average number of messages generated and the average channel busy ratio (CBR) are reported. The CBR indicates the portion of resources that are currently estimated as used by the generic node, with more details provided in Appendix C. In the case of LTE-V2X, the average number of transmissions per packet is also shown in Table II.

If we compare the second group of cases in Table II, which corresponds to the co-channel conditions investigated in the previous subsection, with the first group, which corresponds to either technology alone, we notice that the coexistence impacts more on the CBR of IEEE 802.11p than on the CBR of LTE-V2X. The CBR increase in IEEE 802.11p is higher when the

TABLE II

AVERAGE NUMBER OF MESSAGES (MSG) AND AVERAGE CBR (CBR) FOR IEEE 802.11p and LTE-V2X. IN LTE-V2X, THE AVERAGE NUMBER OF TRANSMISSIONS (NTX) PER PACKET IS ALSO SHOWN.

	50+50 v/km				100+100 v/km					150+150 v/km					
	IEEE	802.11p	LTE-V2X			IEEE 802.11p		LTE-V2X			IEEE 802.11p		LTE-V2X		
Case	Msg	CBR	Msg	Ntx	CBR	Msg	CBR	Msg	Ntx	CBR	Msg	CBR	Msg	Ntx	CBR
IEEE 802.11p only	4.87	0.055				4.84	0.107				4.89	0.166			
LTE-V2X only (w/preamble)			4.86	2	0.17			4.83	2	0.316			4.88	2	0.446
Coexistence legacy	4.88	0.192	4.79	2	0.3	4.89	0.358	4.81	2	0.52	4.89	0.496	4.85	1.99	0.684
Legacy w/ periodic generation	5	0.21	5	2	0.343	5	0.405	5	2	0.617	5	0.532	5	1.87	0.770
W/preamble	4.88	0.401	4.79	2	0.322	4.61	0.635	4.81	2	0.542	2.73	0.781	4.85	2	0.626
W/preamble, no HARQ	4.88	0.245	4.79	1	0.242	4.89	0.426	4.81	1	0.438	4.87	0.568	4.85	1	0.598
W/preamble, half pool	4.88	0.343	4.79	1.97	0.308	4.89	0.491	4.81	1.98	0.516	4.89	0.579	4.85	1.98	0.662
W/preamble, modified LTE CC	4.88	0.351	4.74	1.72	0.294	4.89	0.399	4.15	1.11	0.422	4.89	0.493	3.81	1.02	0.564

preamble insertion is introduced and this is motivated by the presence of a larger protected area, which is an aspect that has been thoroughly discussed in Section IV.

If the attention is focused on scenarios with large density (i.e., 150+150 v/km), it can be observed that in the case of the preamble insertion the congestion control (CC) reduces the average messages generated in IEEE 802.11p to less than 3 per station per second; this eventually causes the DA to increase, as observed in Fig. 7(c).

E. Approaches to manage the congested cases

As already observed with reference to the first two bars of the series in Fig. 7, when the density of vehicles increases, LTE-V2X stations tend to use most of the resources, the preamble tends to be insufficient to mitigate the coexistence issues, and eventually the IEEE 802.11p traffic is reduced by its CC mechanism. For this reason, the following three approaches are considered in addition to preamble insertion to avoid that LTE-V2X stations take most of the channel:

- No HARQ: the use of blind retransmissions is inhibited in LTE-V2X; this avoids that LTE-V2X stations perform two transmissions per packet, thus making the traffic generated by the two technologies similar;
- *Half pool:* LTE-V2X stations are allowed to use only a portion of the subframes; this approach, also discussed in [6], [7], is allowed in LTE-V2X thanks to the concept of pool of accessible resources; a pool of 25 subframes every 50 ms is supposed (corresponding to 50%);
- Modified LTE CC, the CC defined in [26] is altered to reduce the use of the channel by LTE-V2X; in particular, all the thresholds controlling the channel occupation are halved, as detailed in Appendix C. We adopted exactly half for all thresholds as a simple solution. The optimization of the CC mechanism is beyond the scope of the present paper and left for future work.

The impact of the three approaches in terms of generated messages and channel occupation is observable in Table II, while the PRR and DA are shown in Fig. 7.

Regarding no HARQ, Table II shows that it reduces the number of transmissions per message in LTE-V2X to one and this allows IEEE 802.11p to maintain around 4.9 average messages per station per second even with 150+150 v/km. This also allows a significant improvement of the PRR of IEEE 802.11p, as shown in Fig. 7(a). At the same time, LTE-V2X

cannot exploit one of its features, which implies a significant performance loss even when not necessary.

Moving to the half pool, which is also of straightforward implementation, it still allows both technologies to maintain the same average messages per station per second even in the denser case (see Table II); however, as observable in Figs. 7(a)-7(b), the PRR of IEEE 802.11p is improved only when the vehicle density is low. Moreover, the PRR of LTE-V2X is always smaller than that of the legacy and with preamble insertion. This effect is due to the fact that even if LTE-V2X stations leave half of the subframes free to be used by IEEE 802.11p, the average number of LTE-V2X transmissions performed within the allowed pool is doubled, with negative impact on both technologies.

The last solution, which is to modify the CC of LTE-V2X, shows the best performance for IEEE 802.11p under high density conditions. The performance reduction of LTE-V2X compared to legacy and with preamble insertion is similar to the other two approaches, with a DA which is better than no HARQ for low vehicle density and of half pool in all the cases.

Generally, it can be observed that an improvement in one technology corresponds to a performance loss in the other. However, adopting the preamble insertion with a modification of the CC mechanisms of LTE-V2X allows to maintain nearly best performance for both technologies in low density conditions and provides a better balance between the performances of the two technologies when the density increases.

VI. CONCLUSION

In this work, focusing on a scenario where IEEE 802.11p and sidelink LTE-V2X Mode 4 coexist in the same geographical area and in the same channel, we have investigated the insertion of the IEEE 802.11p preamble at the beginning of the LTE-V2X transmissions to mitigate the reciprocal intertechnology interference. Such a preamble insertion requires no modifications to IEEE 802.11p, therefore being retrocompatible with current deployments in Europe, and implies only minor modifications to the LTE-V2X devices. We have first derived an analytical model to investigate the impact in free-flow scenarios, which has lead to a closed-form expression demonstrating the significant reduction of the occurring collisions. Then, large-scale simulations adopting an open-source platform were performed to investigate denser scenarios, confirming the effectiveness of the proposal. Overall,

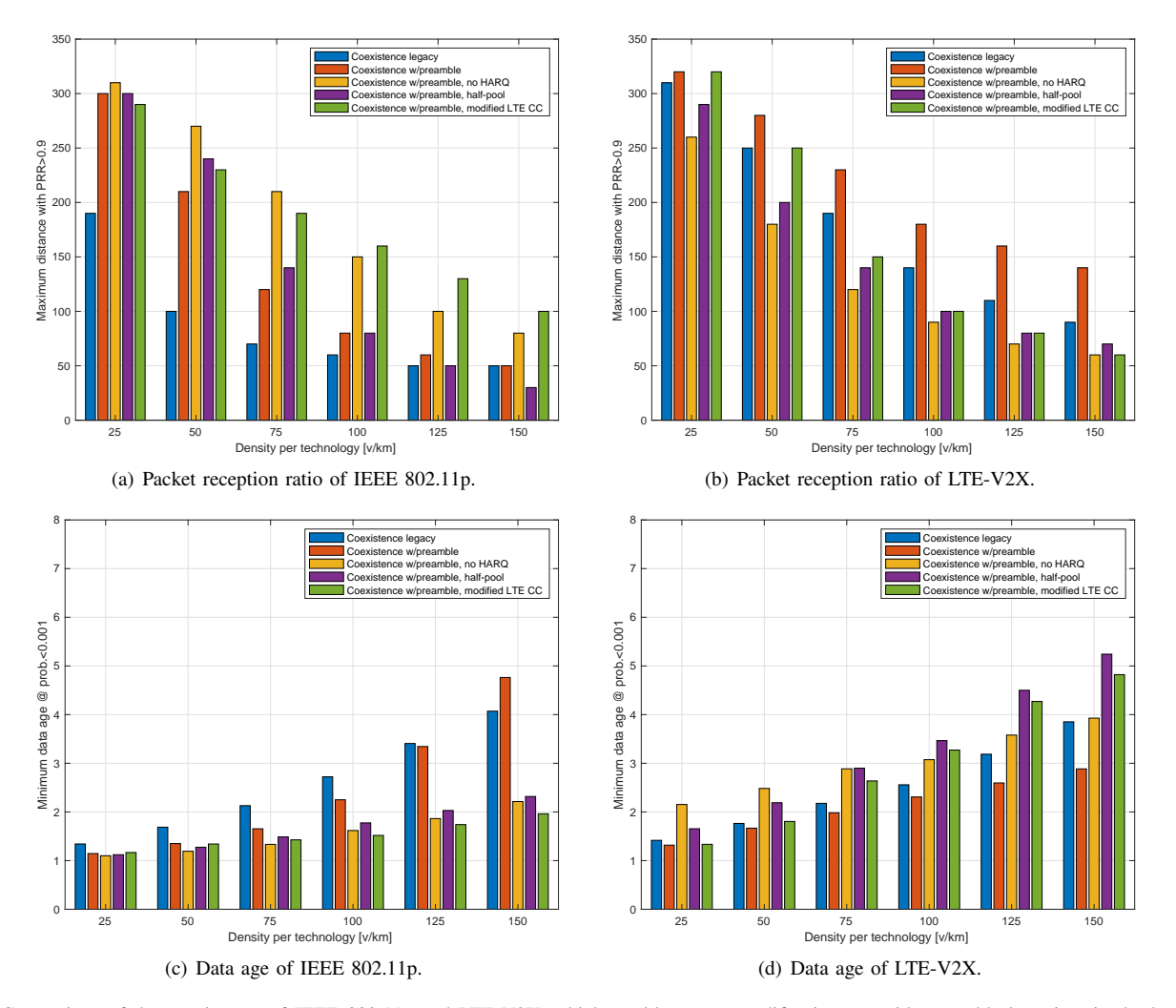


Fig. 7. Comparison of the coexistence of IEEE 802.11p and LTE-V2X vehicles, without any modifications or with preamble insertion, in the latter case without or with additional limitations.

the solution based on preamble insertion has reduced the performance loss caused by co-channel coexistence, without impacting on the performance of either technology when deployed alone. It has also been shown that the mitigation losses effectiveness under high channel load conditions, since LTE-V2X tends to have higher access to the channel. Among three different approaches proposed to limit this effect, the one acting on the congestion control algorithm of LTE-V2X has been shown to be the most effective one.

APPENDIX A: DERIVATION OF (4)

The PRP, given that the main interferer is outside the protected range, is

$$\mathbb{P}_{\text{PR}|\text{busy}} = \frac{1}{1 - \mathbb{P}_{\text{busy}}} \int_{\mathbb{R} - \{\mathbb{S}\}} \mathbb{P}_{\text{d}}(x) f_{\text{PER}}\left(\frac{P_{\text{R}}}{P_{\text{N}} + P_{\text{LTE}} G_{\text{t}} G_{\text{r}} / L(x)}\right) dx$$
(11)

where $\mathbb S$ is the interval within the protected range, i.e., from $d_{\rm u}-d_x^*$ to $d_{\rm u}+d_x^*$ and $\mathbb R-\{\mathbb S\}$ indicates from $-\infty$ to ∞ except $\mathbb S$. The term before the integral in (11) is a normalization due to the assumption to have the LTE-V2X interferer outside the protected area and the integrand represents the conditioned PRP for the possible positions of the interferer.

Approximating, as stated in Section IV-A, the $f_{\rm PER}(\gamma)$ to a threshold curve, the threshold SINR corresponds to a maximum interference value above which the packet is lost, which in turn corresponds to the minimum distance for the interferer d_i . Under this approximation, (11) can be written as

$$\mathbb{P}_{\text{PR}|\text{busy}} = \frac{1}{1 - \mathbb{P}_{\text{busy}}} \left[\int_{-\infty}^{-\max\{\underline{d_i}, (d_x^* - d_u)\}} \mathbb{P}_{\mathbf{d}}(x) dx + \int_{\max\{\underline{d_i}, (d_x^* + d_u)\}}^{\infty} \mathbb{P}_{\mathbf{d}}(x) dx \right]$$
(12)

which leads to (4).

APPENDIX B: DERIVATION OF (8) AND (9)

In the case that the current TTI is sensed idle by the IEEE 802.11p transmitter and the transmission ends in the subsequent TTI, the PRP is equal to

$$\mathbb{P}_{\text{PR}|\text{sq}} = \frac{1}{1 - \mathbb{P}_{\text{busy}}} \int_{0}^{1} \left[\int_{-\infty}^{\infty} \mathbb{P}_{\text{d}}(y) \right] \cdot \left[\int_{\mathbb{R} - \{\mathbb{S}\}} \mathbb{P}_{\text{d}}(x) f_{\text{xy}}(x, y, \tau) dx \right] dy d\tau . \quad (13)$$

where

$$f_{xy}(x, y, \tau) = f_{PER} \left(\frac{P_{R}}{P_{N} + (1 - \tau) \frac{P_{LTE} G_{t} G_{r}}{L(x)} + \tau \frac{P_{LTE} G_{t} G_{r}}{L(y)}} \right)$$
(14)

and the variable τ indicates the portion of the packet transmitted during the subsequent TTI. By assuming that the interference is entirely caused by the LTE-V2X transmission that overlaps most with the reference transmission (i.e., the one in the current TTI if $\tau < 0.5$ and the one in the subsequent TTI if $\tau \geq 0.5$), (13) can be approximated as

$$\mathbb{P}_{PR|sq} = \frac{1/2}{1 - \mathbb{P}_{busy}} \left[\int_{\mathbb{R} - \{S\}} \mathbb{P}_{d}(x) f_{PER} \left(\frac{P_{R}}{P_{N} + P_{LTE} G_{t} G_{r} / L(x)} \right) dx \right]
+ \frac{1}{2} \int_{-\infty}^{\infty} \mathbb{P}_{d}(y) f_{PER} \left(\frac{P_{R}}{P_{N} + P_{LTE} G_{t} G_{r} / L(y)} \right) dy
= \frac{\mathbb{P}_{PR|busy}}{2} + \frac{\mathbb{P}_{PR|unpr}}{2}$$
(15)

where

$$\mathbb{P}_{\text{PR}|\text{unpr}} = \int_{-\infty}^{\infty} \mathbb{P}_{\text{d}}(y) f_{\text{PER}} \left(\frac{P_{\text{R}}}{P_{\text{N}} + P_{\text{LTE}} G_{\text{t}} G_{\text{r}} / L(y)} \right) dy . \tag{16}$$

Directly, (15) corresponds to (8). Furthermore, from (16), by applying the threshold model for the PER vs. SINR, we obtain

$$\mathbb{P}_{\text{PR}|\text{unpr}} = \int_{-\infty}^{-\underline{d_i}} \mathbb{P}_{d}(y) dy + \int_{d_i}^{\infty} \mathbb{P}_{d}(y) dy$$
 (17)

which leads to (9).

APPENDIX C: CONGESTION CONTROL

In Section V, the CC mechanisms described in [24] and [26] are used for IEEE 802.11p and LTE-V2X, respectively.

- 1) IEEE 802.11p: distributed congestion control (DCC) detailed for ITS-G5 in [24]; each station measures the portion of time during which the received power is above -85 dBm, within intervals of 100 ms, called CBR and here denoted as $\delta_{\text{CBR-11p}}$; denoting as t_g the generation interval between a packet and the next one as indicated by the higher layers from [21], the interval used between consecutive packets is calculated as $t_{\Delta} = \max\{t_g, \min\{1, t_g \cdot 4000 \cdot \frac{\delta_{\text{CBR-11p}} 0.62}{\delta_{\text{CBR-11p}}}\}\}$, where $\min\{x,y\}$ is a function that returns the minimum value between x and y. If the CBR goes above 0.62, the generation interval is increased in order to reduce the channel occupation.
- 2) LTE-V2X: CC detailed in [26]; each station measures every 100 ms the portion of subchannels with received power above -94 dBm, called CBR and here denoted as $\delta_{\text{CBR-LTE}}$; based on this and using the settings for the cooperative awareness messages (CAMs), the average number of subchannels that can be used per second by the station, called channel occupation ratio (CR) and here denoted as $\rho_{\text{CR-LTE}}$, is constrained to $\rho_{\text{CR-LTE}} < 0.03$ if $0.3 < \delta_{\text{CBR-LTE}} \le 0.65$, $\rho_{\text{CR-LTE}} < 0.006$ if $0.65 < \delta_{\text{CBR-LTE}} \le 0.8$, and $\rho_{\text{CR-LTE}} < 0.003$ if $\delta_{\text{CBR-LTE}} > 0.8$. The way to reduce the load is not specified in the standards and various options are possible (e.g., varying the MCS or power). In the simulator, we assume that in order to respect the constrain on the $\rho_{\text{CR-LTE}}$, first blind retransmissions are avoided, and then, if not sufficient, the same equation used for IEEE 802.11p is applied to the generation interval.

3) LTE-V2X with modified CC: same algorithm with stricter constraints; specifically, all numbers are halved, meaning that $\rho_{\text{CR-LTE}} < 0.015$ if $0.15 < \delta_{\text{CBR-LTE}} \leq 0.325$, $\rho_{\text{CR-LTE}} < 0.003$ if $0.325 < \delta_{\text{CBR-LTE}} \leq 0.4$, and $\rho_{\text{CR-LTE}} < 0.0015$ if $\delta_{\text{CBR-LTE}} > 0.4$.

REFERENCES

- [1] L. Polak and J. Milos, "Performance analysis of LoRa in the 2.4 GHz ISM band: coexistence issues with Wi-Fi," *Telecommunication Systems*, pp. 1–11, 2020.
- [2] C. F. Chiasserini and R. R. Rao, "Coexistence mechanisms for interference mitigation in the 2.4-GHz ISM band," *IEEE Transactions on Wireless Communications*, vol. 2, no. 5, pp. 964–975, 2003.
- [3] F. M. Abinader, E. P. L. Almeida, F. S. Chaves, A. M. Cavalcante, R. D. Vieira, R. C. D. Paiva, A. M. Sobrinho, S. Choudhury, E. Tuomaala, K. Doppler, and V. A. Sousa, "Enabling the coexistence of LTE and Wi-Fi in unlicensed bands," *IEEE Communications Magazine*, vol. 52, no. 11, pp. 54–61, 2014.
- [4] B. Mafakheri, L. Goratti, R. Abbas, S. Reisenfeld, and R. Riggio, "LTE/Wi-Fi coordination in unlicensed bands: An SD-RAN approach," in 2019 IEEE Conference on Network Softwarization (NetSoft), 2019.
- [5] A. Bazzi, A. Zanella, I. Sarris, and V. Martinez, "Co-channel coexistence: Let ITS-G5 and sidelink C-V2X make peace," in *IEEE ICMIM*, 2020, pp. 1–4.
- [6] P. Roux and V. Mannoni, "Performance Evaluation for Co-channel Coexistence Between ITS-G5 and LTE-V2X." in *IEEE VTC Fall 2020*.
- [7] "Intelligent transport systems (ITS); pre-standardization study on cochannel co-existence between IEEE- and 3GPP-based its technologies in the 5 855 MHz-5 925 MHz band," ETSI TR 103 766 v1.1.1, Sept. 2021.
- [8] "IEEE 802.11-2020 IEEE standard for information technology telecommunications and information exchange between systems local and metropolitan area networks-specific requirements part 11: Wireless lan medium access control (MAC) and physical layer (PHY) specifications," IEEE, 2020.
- [9] M. Sepulcre, J. Gozalvez, and B. Coll-Perales, "Why 6 Mbps is not (always) the optimum data rate for beaconing in vehicular networks," *IEEE Transactions on Mobile Computing*, vol. 16, no. 12, pp. 3568– 3579, Dec 2017.
- [10] C. Campolo, A. Molinaro, A. Vinel, and Y. Zhang, "Modeling prioritized broadcasting in multichannel vehicular networks," *IEEE Transactions on Vehicular Technology*, vol. 61, no. 2, pp. 687–701, Feb 2012.
- [11] A. Bazzi, A. Zanella, and B. M. Masini, "Optimizing the resource allocation of periodic messages with different sizes in LTE-V2V," *IEEE Access*, pp. 1–1, 2019.
- [12] A. Bazzi, G. Cecchini, A. Zanella, and B. M. Masini, "Study of the impact of PHY and MAC parameters in 3GPP C-V2V mode 4," *IEEE Access*, pp. 1–1, 2018.
- [13] R. Molina-Masegosa, J. Gozalvez, and M. Sepulcre, "Configuration of the C-V2X Mode 4 sidelink PC5 interface for vehicular communications," in MSN 2018.
- [14] B. Toghi, M. Saifuddin, H. N. Mahjoub, M. Mughal, Y. P. Fallah, J. Rao, and S. Das, "Multiple access in cellular V2X: Performance analysis in highly congested vehicular networks," in 2018 IEEE Vehicular Networking Conference (VNC). IEEE, 2018, pp. 1–8.
- [15] "Intelligent transport systems (ITS); access layer specification for intelligent transport systems using lte vehicle to everything communication in the 5,9 ghz frequency band," ETSI TS 103 613 V1.1.1, 2018.
- [16] Z. Tong, H. Lu, M. Haenggi, and C. Poellabauer, "A stochastic geometry approach to the modeling of DSRC for vehicular safety communication," *IEEE Transactions on Intelligent Transportation Systems*, vol. 17, no. 5, pp. 1448–1458, 2016.
- [17] W. Zhang, Y. Chen, Y. Yang, X. Wang, Y. Zhang, X. Hong, and G. Mao, "Multi-hop connectivity probability in infrastructure-based vehicular networks," *IEEE JSAC*, vol. 30, no. 4, pp. 740–747, May 2012.
- [18] A. Bazzi, A. Zanella, G. Cecchini, and B. M. Masini, "Analytical investigation of two benchmark resource allocation algorithms for LTE-V2V," *IEEE Transactions on Vehicular Technology*, vol. 68, no. 6, pp. 5904–5916, June 2019.
- [19] Y. Park, T. Kim, and D. Hong, "Resource size control for reliability improvement in cellular-based V2V communication," *IEEE Transactions* on Vehicular Technology, pp. 1–1, 2018.
- [20] "Technical specification group radio access network; study on LTE-based V2X services," 3GPP TR 36.885 V14.0.0, July 2016.

- [21] "Intelligent transport systems (ITS); vehicular communications; basic set of applications; part 2: Specification of cooperative awareness basic service," *3GPP EN 302.637-2 V1.3.1*, September 2014.
 [22] "Survey on ITS-G5 CAM statistics," CAR 2 CAR Communication
- Consortium, TR2052, 2018.
- [23] "Intelligent transport systems (ITS); vehicular communications; GeoNetworking; part 4: Geographical addressing and forwarding for pointto-point and point-to-multipoint communications; sub-part 2: Mediadependent functionalities for ITS-G5," ETSI TS 102 636-4-2, 2013.
- [24] "Intelligent transport systems (ITS); ITS-G5 access layer specification for intelligent transport systems operating in the 5 GHz frequency band," ETSI EN 302 663, 2020.
- [25] S. Bartoletti, B. M. Masini, V. Martinez, I. Sarris, and A. Bazzi, "Impact of the generation interval on the performance of sidelink C-V2X autonomous mode," IEEE Access, vol. 9, pp. 35121-35135, 2021.
- [26] "Intelligent transport systems (ITS); congestion control mechanisms for the C-V2X PC5 interface; access layer part," ETSI TS 103 574 V1.1.1, Nov. 2018.
- [27] V. Todisco, S. Bartoletti, C. Campolo, A. Molinaro, A. O. Berthet, and A. Bazzi, "Performance analysis of sidelink 5G-V2X mode 2 through an open-source simulator," IEEE Access, vol. 9, 2021.